Measuring Economic Growth With A Fully Identified Three-Signal Model

Andrea Civelli* Arya Gaduh† Ahmed Sadek Yousuf ‡

University of Arkansas *University of Arkansas, NBER* *Aix-Marseille School of Economics*

Abstract

We augment Henderson, Storeygard, and Weil (2012)'s two-signal model of true income growth with a third signal to overcome its underidentification problem. The additional moment conditions from the third signal help fully identify all model parameters without ad-hoc calibrations of the GDP's signal-to-noise ratio. We characterize the necessary properties of the third signal. Using the model, we recover the optimal weight of the GDP in the composite economic growth estimates, which varies with the quality of the national statistics and the geographic level of analysis. The model improves on existing methodologies that use signals to measure true income.

Keywords: Remote sensing; Nighttime lights; Urban expansion; Economic activity measurement.

JEL Classification: E01, O11, O47, O57.

*University of Arkansas, Walton College of Business, Department of Economics, Business Building 402, Fayetteville, AR. Email: andrea.civelli@gmail.com.

†University of Arkansas, Walton College of Business, Department of Economics, Business Building 402, Fayetteville, AR. Email: agaduh@walton.uark.edu.

‡Email: ahmed-sadek.yousuf@univ-amu.fr.

1 Introduction

The seminal paper of Henderson et al. (2012) (HSW, henceforth) introduced a statistical framework to use changes in nightlights as a useful proxy for economic activity. HSW use this framework to obtain two main results. First, they show that nightlights can be used to directly predict GDP growth. This is useful, for instance, at sub- or supra-national level when official GDP measures are not available. A large body of literature has exploited this result for a variety of empirical applications.[1]

Second, they propose a model that combines GDP — intended as a noisy signal of true economic growth — with nightlights as a second signal to improve estimates of unobservable true income growth. This is particularly useful when official GDP measures exist, but there are reasons to believe they are unreliable. Their two-signal model of true income growth, however, has an important shortcoming: it needs to identify four structural parameters with only three sample moments from observed data. HSW solve this by assuming a value for the signal-to-noise ratio of the GDP signal.

The need for underlying conventional income data and the lack of a straightforward identification strategy have restricted the empirical applications of this model. Nevertheless, estimating true income is, in principle, more relevant than just estimating GDP, and a fully identified model can constitute a useful benchmark for other approaches that aim to measure economic activity. To this end, this paper proposes a novel solution that overcomes the underidentification problem of the HSW framework by augmenting their model with a third signal.

Our results are threefold. First, we theoretically demonstrate that a three-signal version of the HSW model is fully identified. The third signal increases the number of parameters to be estimated; however, it also provides three additional

[1] See, among the others, Storeygard (2016); Michalopoulos and Papaioannou (2013a,b); Alesina et al. (2016); Dreher and Lohmann (2015); Civelli et al. (2018); Hodler and Raschky (2014).

moment conditions, namely its variance and the covariances with the two original signals (official GDP and nightlights). The six moment conditions fully identify the six model parameters. We also characterize the necessary properties of this third signal.

Second, we show how urban land cover data can be a suitable third signal. Globally, urban land cover data have become increasingly available for extended periods and at different frequencies. They have been shown to meaningfully provide information about economic growth beyond night luminosity, especially in more agriculture-intensive regions and at the subnational level (see, for instance, Goldblatt et al., 2019; Keola et al., 2015; Wu et al., 2013). We show its potential as a third signal by estimating the predictive GDP growth regression on changes in nightlights and urban land cover for three sets of aggregate economies: all countries, African countries, and counties within the United States. We find that changes in urban land cover have a significant predictive power of GDP growth, which gets stronger in lower income areas. Overall, while the change in urban land cover cannot be used as a primary signal, it is an ideal candidate for an auxiliary third signal.

Third, we apply the urban land cover change to the augmented model and demonstrate its use to fully identify the model for the estimation of economic growth. We first show that the urban land cover change satisfies the necessary properties of a third signal for our applications. We find that the relative weight of the GDP data in the true income composite (λ^* in the HSW notation adopted here too) is 0.60 for the full set of countries. This weight drops to 0.20 for the sub-group of countries with low-quality official GDP data and increases to 0.88 for countries with high-quality ones. We also find a weight of 0.54 for African countries and 0.70 for the U.S. counties. Overall, these results suggest that the weight assigned to the GDP data by this methodology are inversely related to the reliability of the official GDP data and also depends on the geographic level of analysis.

We then show its empirical applications to illustrate three advantages of our approach. First, we show that when feasible, the three-signal model is superior to simply using the additional signal as a covariate to improve the *predicted GDP growth* (as in e.g., Baragwanath et al., 2021; Engstrom et al., 2021; Goldblatt et al., 2019; Lehnert et al., 2020). We find that the true income-growth estimate from a fully identified model is invariant to adding a third signal to predict GDP growth. Second, the fully identified model introduces new ways to improve income estimates. For example, the identified primitives for a set of regions where an appropriate third signal is available can be used to estimate true income growth in similar regions where such a signal is unavailable.[2] Finally, our approach can be used to validate the use of nightlights or other types of signals to predict economic activities, by providing a useful tool to assess the magnitude and direction of potential measurement errors. We find that these errors can be quite large, especially at the extremes of the income distribution and when true income growth is negative.

We contribute to the literature on methodological improvements to the HSW framework in using signals to measuring true income growth. A strand of this literature highlights the non-linear aspects of the relation between nightlights and underlying economic activity (Bickenbach et al., 2016; Bluhm and McCord, 2022; Chen and Nordhaus, 2011; Goldblatt et al., 2019; Keola et al., 2015; Maldonado, 2022; Wu et al., 2013). Another focuses on the utility of different sources of nightlight data and other satellite data – especially in conjunction with machine learning methodologies – to improve measures of growth (Baragwanath et al., 2021; Beyer et al., 2018; Dai et al., 2017; Engstrom et al., 2021; Gibson and Boe-Gibson, 2021; Goldblatt et al., 2019; Lehnert et al., 2020; Wang et al., 2019; Zhang and Gibson, 2022). The full identification of the model parameters to solve for the true income

[2]This requires an assumption (used by HSW, in their calibration exercise, see p. 1009, 1018) that these two region groupings only differ from one other in their signal-to-noise ratio of the official GDP data.

growth is a novel approach to improve the method.

At the same time, our approach provides a simple tool to aid empirical studies that uses nightlights to estimate socioeconomic developments. The list of topics that have been studied empirically based on nightlights data is long and growing.[3] Our approach provides a simple methodology to fully implement the HSW model in a way that minimizes the uncertainty around the optimal estimate of economic activity produced by the model. This is of paramount importance for all types of empirical applications.

The rest of the paper is organized as follows. Section 2 begins with the original two-signal model of HSW, followed by our proposed refinement using a third signal. In Section 3, we describe the data, show empirical implementations of our model, and illustrate its value for empirical work. We conclude in Section 4.

2 A Three-Signal Model of Economic Activities

2.1 The Underidentification of the Two-Signal Model

To motivate our model, we briefly recapitulate HSW's original model that estimates the true, but unobservable, economic growth by exploiting two observable noisy signals correlated with the true economic activities. Let y_j be the true growth rate in country j. Let g_j and l_j respectively indicate the two signals used in the model, which correspond to the growth rates of real GDP and of observed lights in country j in the empirical exercise. HSW assume that the two signals are linearly related to true economic activities which, as standard in the signal extraction liter-

[3]Nightlights have been employed, among others, to validate statistical measures of income, such as the Penn's World Tables or household surveys (Pinkovskiy and Sala-i Martin, 2016a,b); to estimate informal economic activities (Chen and Nordhaus, 2011; Ghosh et al., 2010); to study the effects of intercity linkages, institutions and ethnic characteristics on regional income in Africa (Alesina et al., 2016; Michalopoulos and Papaioannou, 2013a,b; Storeygard, 2016); to explore regional political favoritism (Hodler and Raschky, 2014); and to estimate the impact of aid on growth at sub-national level (Civelli et al., 2018; Dreher and Lohmann, 2015).

ature, allows for an error orthogonal to y_j that embeds the precision (or tightness) of the signal around the fundamental, namely:

$$g_j = y_j + \varepsilon_{1,j} \tag{1}$$

$$l_j = \beta_l y_j + \varepsilon_{2,j} \tag{2}$$

The variance of y_j is denoted by σ_y^2. Similarly, the variances of the signals are given by σ_g^2 and σ_l^2. A similar notation is used for the variances of the signal noises as well: σ_1^2 and σ_2^2 for $\varepsilon_{1,j}$ and $\varepsilon_{2,j}$.

HSW complete the model with a predictive equation that links the two signals to each other:

$$g_j = \psi_l l_j + e_j. \tag{3}$$

The predicted value $\hat{g}_j = \hat{\psi}_l l_j$ is linearly combined with the observed signal g_j to improve the accuracy of the estimate of the true economic growth exploiting the information contained in the signals:

$$\hat{y}_j = \lambda g_j + (1 - \lambda)\hat{g}_j. \tag{4}$$

The optimal weight on the official GDP, λ^*_{HSW}, in the linear combination in equation (4) is chosen to minimize the variance of the forecast error of the predicted economic growth, i.e., to minimize $var(\hat{y} - y)$, given the structure of the model and the assumption that the errors in equations (1)-(2) are mutually orthogonal.

HSW show that λ^*_{HSW} is a function of four unknown parameters, namely $(\sigma_y^2, \sigma_1^2, \sigma_2^2, \beta_l)$. From equation (8) of HSW, the solution is:

$$\lambda^*_{HSW} = \frac{1}{1 + \left(\frac{\sigma_1^2}{\sigma_y^2} + \frac{\sigma_1^2}{\sigma_2^2}\beta_l^2\right)}. \tag{5}$$

However, only three moment conditions are available from the observable data. Two conditions are obtained from the variance of the signals:

$$\sigma_g^2 = \sigma_y^2 + \sigma_1^2$$
$$\sigma_l^2 = \beta_l^2 \sigma_y^2 + \sigma_2^2,$$

while the last one is provided by the covariance between the two signals, σ_{gl}:

$$\sigma_{gl} = \beta_l \sigma_y^2$$

To close the model and solve for the true income growth, they make use of the signal-to-noise ratio associated with signal g_j, the officially measured GDP growth rate. From equation (1), define the signal-to-noise ratio as:

$$\phi = \frac{\sigma_y^2}{\sigma_y^2 + \sigma_1^2}. \tag{6}$$

HSW split the sample of developing countries into two groups based on the quality of their national accounting system, and assume they only differ by the signal-to-noise ratio, ϕ. If ϕ for one group (say, those with high-quality data) is known, they can use this equation to infer the ϕ for the other, and the optimal λ^*_{HSW}'s for both groups. HSW's preferred estimates of true income growth assume $\phi = 0.9$ for the high-quality data countries and conduct an insightful investigation of the relation between signal precision and λ^*_{HSW}; nevertheless, the underlying identification issue remains as any ϕ would in principle be admissible.

2.2 A Third Signal to Solve Them All

We demonstrate below that the introduction of a third signal can overcome the underidentification of model parameters and do away with the need to assume a value for ϕ. Let the third signal be u_j, corresponding to the growth rate of urban

land cover in the empirical exercise in Section 3. We modify the structure of the model in two ways. First, we add to (1) and (2) an observation equation for the new signal:

$$u_j = \beta_u y_j + \varepsilon_{3,j}. \tag{7}$$

We denote the variance of u_j and $\varepsilon_{3,j}$ with σ_u^2 and σ_3^2 respectively.

Second, the predictive equation (3) is modified to also include the third signal:

$$g_j = \psi_l l_j + \psi_u u_j + e_j, \tag{8}$$

which is associated to a predicted value of the main signal given by $\hat{g}_j = \hat{\psi}_l l_j + \hat{\psi}_u u_j$.

As for the two-signal model, the optimal λ^* of the augmented model is chosen to minimize the variance of the forecast error of the predicted economic growth. Using (8) in (4), $var(\hat{y} - y)$ can be written as

$$\begin{aligned} var(\hat{y} - y) &= var\big[\lambda(g_j - y_j) + (1-\lambda)(\hat{g}_j - y_j)\big] \\ &= \lambda^2\sigma_1^2 + (1-\lambda)^2\big[\hat{\psi}_l^2\sigma_2^2 + \hat{\psi}_u^2\sigma_3^2 + (\hat{\psi}_l\beta_l + \hat{\psi}_u\beta_u - 1)^2\sigma_y^2\big], \end{aligned}$$

where use has been done of the structural equations of the model (1)-(2) and (7) and of the assumption that their errors are mutually orthogonal. After taking the derivative of this expression with respect to λ, we obtain:

$$\lambda^* = \frac{\hat{\psi}_l^2\sigma_2^2 + \hat{\psi}_u^2\sigma_3^2 + \big(\hat{\psi}_l\beta_l + \hat{\psi}_u\beta_u - 1\big)^2\sigma_y^2}{\sigma_1^2 + \hat{\psi}_l^2\sigma_2^2 + \hat{\psi}_u^2\sigma_3^2 + (\hat{\psi}_l\beta_l + \hat{\psi}_u\beta_u - 1)^2\sigma_y^2}. \tag{9}$$

It is easy to show that the OLS estimates $\hat{\psi}_l$ and $\hat{\psi}_u$ return a biased estimate of the inverse of the two coefficients β_l and β_u, with a bias structure that depends

on the underlying parameters of the signaling model.[4] Using this fact and after a few manipulations, λ^* in (9) can be simply expressed as:

$$\lambda^* = \frac{1}{1 + \left(\frac{\sigma_1^2}{\sigma_y^2} + \frac{\sigma_1^2}{\sigma_2^2}\beta_l^2 + \frac{\sigma_1^2}{\sigma_3^2}\beta_u^2\right)}. \tag{10}$$

Therefore, the optimal λ^* depends on six unknown parameters $(\sigma_y^2, \sigma_1^2, \sigma_2^2, \sigma_3^2, \beta_l, \beta_u)$. Six sample moment conditions are necessary to fully identify these six parameters from the data.

The first three condition are obtained from the variance of the three signals, which using (1)-(2) and (7) can be expressed as:

$$\sigma_g^2 = \sigma_y^2 + \sigma_1^2 \tag{11}$$

$$\sigma_l^2 = \beta_l^2\sigma_y^2 + \sigma_2^2 \tag{12}$$

$$\sigma_u^2 = \beta_u^2\sigma_y^2 + \sigma_3^2. \tag{13}$$

The other three conditions are provided by the covariances between the three signals. These can be expressed as:

$$\sigma_{gl} = \beta_l\sigma_y^2 \tag{14}$$

$$\sigma_{gu} = \beta_u\sigma_y^2 \tag{15}$$

$$\sigma_{lu} = \beta_l\beta_u\sigma_y^2 \tag{16}$$

[4]The bias structure is given by:

$$plim(\hat{\psi}_l) = \frac{1}{\beta_l}\left(\frac{\beta_l^2\sigma_y^2\sigma_3^2}{\beta_l^2\sigma_y^2\sigma_3^2 + \beta_u^2\sigma_y^2\sigma_2^2 + \sigma_2^2\sigma_3^2}\right)$$
$$plim(\hat{\psi}_u) = \frac{1}{\beta_u}\left(\frac{\beta_u^2\sigma_y^2\sigma_2^2}{\beta_l^2\sigma_y^2\sigma_3^2 + \beta_u^2\sigma_y^2\sigma_2^2 + \sigma_2^2\sigma_3^2}\right).$$

Conditions (14)-(16) give the solution for β_l, β_u, and σ_y^2. Given these, (11)-(13) allow us to solve for σ_1^2, σ_2^2, and σ_3^2. We explicitly derive the model solution in Appendix A.1.

The third signal provides three new moment conditions — equations (13), (15), and (16) — with the introduction of two additional parameters (β_u and σ_3^2). It therefore overcomes the underidentification issue of the two-signal model. Two of these moment conditions are equivalent to those related to signal l in HSW, and they are respectively obtained from the variance of signal u in (13) and the covariance between this signal and signal g in (15). In addition to these moments, the covariance between u and l in (16) provides the new information that ensures the identification of the model.

The covariance structure of the signals must empirically satisfy a set of necessary conditions for the solution to exists. In particular, the covariance between the second and third signals must be positive and sufficiently strong, i.e.:

$$\sigma_{lu} > 0 \tag{17}$$

$$\sigma_g^2 > \frac{\sigma_{gu}\sigma_{gl}}{\sigma_{lu}}. \tag{18}$$

We detail these conditions in Appendix A.1.

Note that the primary scope of the three-signal model is to overcome the identification shortcoming of the two-signal HSW model. The solution to the three-signal model also allows us to recover the primitive parameters necessary to estimate λ^*_{HSW} for the two-signal model in (5). Hence, we can use equation (6) to infer true growth for the whole sample, even if the additional signal is only informative for a subset of the sample for a given period. The ϕ for the sample where the third signal is informative would be sufficient to also pin down ϕ and λ^*_{HSW} for the rest of the sample. This largely simplifies the search for an empirically suitable third

signal for the full sample in all periods.[5]

Finally, the use of a third signal is suitable as long as two important implicit conditions are satisfied. First, the new signal must be sufficiently informative. This means it must be not only correlated with economic activity, but also with the main signals. Second, the two error terms in equations (2) and (7) are assumed to be uncorrelated. If this condition was not satisfied, then an additional covariance term would be found in the expression for $var(\hat{y} - y)$, and another moment condition would be necessary again. The mutual orthogonality of the errors of the signal equations is a fairly common assumption in signaling models.

3 Urban Land Cover as a Third Signal

In this section, we turn to the empirical implementation of the three-signal model. We begin with a summary of the rich datasets used in our analysis. Then, we examine the properties of the change in urban land cover as a signal to predict GDP growth and compare it with the use of nightlights variations. Finally, we implement our augmented model using nightlights and urban cover to estimate λ^* in equation (10). We consider a sample at the country level for the whole world, comparable to the sample used by HSW, and one for African countries. We explore potential sub-national applications with the U.S. counties.

3.1 Data

3.1.1 Night Lights

Nightlights data are derived from annual composites of nightlights intensity from the Defense Meteorological Satellite Program (DMSP) satellites. The stable lights product provides 6-bit digital numbers (DN) ranging from 0 to 63 for each 30 arc-

[5]See Appendix A.2 for a full derivation of the solution for this split-sample approach.

second output pixel. During processing, ephemeral lights, such as from fires and gas flaring, are removed. Processing also excludes (at the pixel level) images for nights affected by clouds, moonlight, sunlight, and other glare. Lights are aggregated at the geographic level of analysis, after applying a correction for the curvature of the Earth at country level.[6]

We extend the baseline DMSP data, which are based on observations intended to span the day-night boundary and ends in 2013, with the series produced by the Earth Observation Group (Ghosh et al., 2009) for the period 2014-2020 by using pre-dawn nightlights data from F15 and F16 DMSP satellites.[7] Nightlights as observed in the early hours of the morning are likely to stem from largely public infrastructure only, and while certain studies have treated this as separate from the earlier DSMP time-series (for example Gibson and Boe-Gibson, 2021), for our purposes, we use the two time series together. This is because given our methodology revolves around "long-differencing" between two distant points in time, the usage of the extended data would provide a lower bound regarding estimate of elasticity of nightlights. Nevertheless, the estimates of the elasticity we obtain are consistent with those in HSW (see Table 1).

3.1.2 Urban Land Cover

Our measure of urban land cover is obtained from the European Space Agency (ESA) Climate Change Initiative (CCI). Their land cover raster product documents consistent global land cover coverage at 300 meters spatial resolution on an annual basis from 1992 to 2020, describing the land surface in the 22 classes defined by the

[6]Because of the curvature of the Earth, grid cell size varies in proportion to the cosine of latitude. We follow HSW's procedure by calculating a weighted average (based on country's land area) of lights across pixels within a country.

[7]While all DMSP satellites are sun-synchronous polar-orbiting platforms, the timing of DMSP logged observations (overpass) varies. This is because the DMSP satellites have unstable orbits. Thus, while originally the timing of observations was in the early evening (for example, the F18 satellite coverage was at circa 8:30 pm in 2013), the decayed orbit means that the DSMP satellites shifted to earlier overpass times later on.

United Nations Land Cover Classification System (LCCS). We extract the share of urban land cover from the original compound land cover raster data. Similar to nightlights, for the national level analysis, we adjust for the curvature of Earth for this data as well.[8]

3.1.3 GDP

For our national level analysis, official country GDP data at national level are derived from the 2021 World Development Indicators (WDI) dataset of the World Bank. We use constant 2015 US dollar denominated GDP figures. Our US-county data come from the official county-level economic output data of the Bureau of Economic Statistics, U.S. Department of Commerce, and recorded in 2012 U.S. dollars. We restrict our analysis to mainland U.S., excluding Hawaii and Alaska.

3.1.4 Statistical Capacity Score

Similar to HSW, we demarcate the countries used in our analysis based on the robustness of their respective statistical capacities. We use the World Bank's Statistical Capacity Indicators from 2010. It is a composite score that assesses the capacity of a country's statistical system. It is based on a diagnostic framework assessing the following areas: methodology; data sources; and periodicity and timeliness. Countries are scored against 25 criteria in these areas, using publicly available information and/or country input. The overall score is a simple average of all three

[8]In our empirical application, the orthogonality of the errors in equations (2) and (7) reasonably rests on the differences in satellites and technologies from which land cover and nightlights data are obtained. Land cover data primarily come from the elaboration of moderate spatial resolution images produced by the Medium Resolution Imaging Spectrometer (MERIS) as part of the ESA Environmental Satellite Program (Envisat), integrated with complementary sources such as the SPOT (Satellite Pour l'Observation de la Terre)-VEGETATION Programme (Defourny et al., 2017). On the contrary, NOAA elaborates data collected by the Operational Linescan System (OLS) multispectral radiometer on the DMSP satellites, which belong to a program with meteorological and military purposes of the U.S. Space Force (see Elvidge et al., 2004; Henderson et al., 2012, for more information).

area scores on a scale of 0-100. We use a cutoff of 50 to distinguish between countries with high and low statistical capacity.

3.2 GDP Growth Predictive Regressions

We first estimate the real GDP growth, g, predictive regression model (8) in which the growth of nightlights luminosity, l, and urban land cove, u, are used as predictors over long time spans. The growth rates are constructed as log-differences, taking the means of the first and last two years of the period as initial and final observations respectively. Table 1 reports the estimates of the model for the three samples. The predictive regressions are estimated over long time periods of 20-25 years to capture the long-term correlations between economic growth and the signals.

Our methodology is mostly agnostic regarding the predictive stage of the HSW model. It simply requires that an additional informative signal with the aforementioned statistical characteristics regardless of the relative magnitude of its coefficient in model (8). However, it is worth noting that at the country level, especially in the sample with more developing nations, the urban growth coefficient is larger than at the sub-national level. In Africa, the coefficient of the urban land cover growth is more strongly significant than that of the nightlights growth. The model fit, captured by the adjusted R^2, does not necessarily increase with the additional signal.

3.3 Estimating the GDP Growth Weight, λ^*

We turn now to the optimal weight for the official GDP growth, λ^*, in equation (10) for our three samples. Table 2 summarizes the overall results. Appendix Table B.1 reports the full set of estimated parameters and covariance matrices.

3.3.1 All Countries

Our first sample parallels the HSW's exercise. We extend their sample with seventeen countries not included in HSW, but we lose nine due to data limitations.[9] We also extend the time period by about ten years.

We first note that the correlation between l and u is smaller than both the correlations between l and g and between u and g. Nevertheless, it is positive and still relatively sizable, as expected from conditions (17) and (18).[10]

We then estimate a $\lambda^* = .6$ for the entire group of countries. The corresponding signal-to-noise ratio of the GDP signal ϕ in (6) is $.78$. This sample includes a large variety of countries, and we can think of this λ as a broadly defined reference value at national level that would work in general for countries with "average" GDP data quality. As done by HSW, we also split the sample of countries into two sets based on the World Bank classification of the capacity of their national statistical agencies. For the countries with low-quality statistical capacity we obtain $\lambda^* = .20$ and $\phi = .38$, whereas the high-quality ones have $\lambda^* = .88$ and $\phi = .94$.[11]

Our estimates validate the calibration exercise of HSW by showing that the optimal GDP weight λ^* is an increasing function of the GDP data quality and that the luminosity and urban land cover are useful signals to recover the true economic activity when the GDP data is unreliable. However, the major difference — and the contribution — of our approach is that the augmented models for the two groups are independently identified. Our approach does not require an initial guess to calibrate the signal-to-noise ratio of the GDP growth signal for either group. Instead, it allows the data to produce a high λ for the countries with high-quality statistical capacity, implying that their GDP data already provide an excellent proxy for

[9] Appendix Table B.2 lists the included countries and their GDP data quality.

[10] More precisely, the conditions are based on a comparison of variances and covariances of the signals. We prefer to rely on correlations in the discussion here because they provide the intuition and are easier to interpret.

[11] As in HSW, this exercise assumes that the two groups have different signal-to-noise ratios for the GDP growth signal, while the relation between the other two signals and GDP is taken as common across groups.

economic activity.

3.3.2 African Countries

This sample includes developing countries in the lower-mid range of GDP data reliability.[12] As for the full world sample, the correlation between l and u is positive, but smaller than the l-g and u-g correlations. This is consistent with the conditions for the existence of a solution. The optimal estimated weight is $\lambda^* = .54$, with a corresponding signal-to-noise ratio of the GDP growth signal of $\phi = .65$. This result corroborates the intuition of the previous case by showing that the key determinant of λ is the quality of the national accounting system rather than the degree of development of the countries.

3.3.3 U.S. Counties

Our third exercise explores a sub-national case for an advanced economy using U.S. counties. The U.S. national statistical capacity is classified at the highest level of quality, hence we would expect its county-level GDP data to be of a similarly high quality and λ^* to be quite large. Instead, we find $\lambda^* = .7$ – lower than the $.88$ value for the countries with high-quality statistical capacity and more in line with the average weight of $.6$.[13]

This result illustrates how, at the sub-national level, the luminosity and urban land-cover signals may still be relevant even in advanced, high data quality countries. Measuring disaggregated GDP at local level with good precision is more difficult than measuring the overall national GDP. Idiosyncratic components make regional economic activity less homogeneous and more difficult to interpret by a central statistical agency. Moreover, a high-quality national statistical agency

[12] Appendix Table B.3 lists included African countries.

[13] We also note that the contribution of u to the GDP growth prediction is smaller compared to the other two cases. Nevertheless, the correlation with the l signal remains sufficiently strong to allow u to provide a useful signal for the augmented model.

might have to rely on the support of local government agencies, which might not be as well-funded as the national one.

3.4 Discussion: Empirical Implications of the Augmented Model

The main advantage of our approach is it does away with the need for an outside parameter choice to estimate true income growth. We now show its value for empirical work. First, we show that the gains in accuracy when using the HSW model to predict economic activity primarily comes from remedying its lack of identification, rather than from refinements to the GDP growth prediction. In other words, the real gains are obtained by the optimal identification of λ^*. Second, we show that, when it is feasible to estimate the three-signal model, such estimates can be used to validate and assess the magnitude and direction of potential measurement errors of empirical applications of signal-based estimation of economic activities.

3.4.1 Model Accuracy

We first compare the predicted GDP growth from equation (8), $\hat{g}_i$, with the estimated true economic activity growth, $\hat{y}_i$ in (4). Both estimates use the three-signal model specification. We calculate the root mean squared error (RMSE) of using $\hat{g}_i$ instead of $\hat{y}_i$ to predict growth in the full sample of countries. We find an RMSE of 21% — a large error that is a quarter of the average estimated $\hat{y}_i = 84\%$ over the 24 years of our sample.

Next, we show that adding the urban signal in the predictive stage leads to a negligible gain in accuracy. After estimating the parameters from the fully identified model, we estimate $\hat{y}_i$ using the three-signal predicted GDP (equation 8) and the two-signal predicted GDP (equation 3). The scatter plot in Figure 1 compares the two series for all countries. The two estimates are very similar. They positively comove and a formal t-test does not reject the hypothesis that the difference between the two is zero (with p-value = 1). This indicates that the gain in accuracy

from adding an extra signal in the predictive stage is marginal compared to that from properly identifying λ^*.

Finally, we show that achieving full identification is paramount for the accuracy of the economic growth estimates by estimating $\hat{y}_i$ for the countries with low-quality statistical capacity using the overall $\lambda^* = .60$ instead of the group-specific parameter $.20$. We find that this alternative growth prediction would incur an RMSE of 14%, which corresponds to about one sixth of the average growth of 82% estimated for this sample of countries with the correct weights.

Notably, as an additional benefit, combining our approach with the HSW's split-sample strategy can provide a convenient way to estimate economic activity for a set of countries with a fully identified model even if a third signal is not directly available. Under the assumption that two set of countries differ only in terms of their signal-to-noise ratios of the GDP growth signal, the availability of a third signal for one group of countries is sufficient to also identify σ_y and λ^*_{HSW} (the optimal weight for the two-signal model) for the other group. This λ^*_{HSW} would allow us to construct an estimate of economic activity growth only relying on the nightlights signal which, as demonstrated above, is fairly close to that obtained from the augmented model.

3.4.2 Model Validation and Measurement Errors

A common empirical application of the HSW framework is to use the predictive stage to estimate GDP growth from nightlights changes. The baseline $\hat{\psi}_l = .3$ found by HSW is sometimes used; alternatively, when official income data are available for a subset of countries or regions, the predictive model is fitted and the estimated $\hat{\psi}_l$ applied to the remaining part of the sample (see e.g., Civelli et al., 2018).

We can use true income growth estimates from the augmented model to assess this practice by comparing the predicted GDP growth, $\hat{g}$, to the true income growth, $\hat{y}$. First, we randomly select two thirds of a sample as a training sample

to estimate $\hat{\psi}_l$. We then use it to predict the GDP growth for the remaining third of "out-of-sample" observations. We repeat these steps for one hundred times and take the average predicted GDP growth for each geographic unit. As a proof of concept, we work with the full African countries sample and the counties in Texas. Figure 2 present these comparisons with African countries in Panel (a), grouped by quality of the official GDP data, and Texan counties in Panel (b), with a separate color for those in the Rio Grande Valley (along the southern border with Mexico).

The results for the African countries show that the predicted GDP growth generally underestimates the true income growth, with the exception of five lower-quality and one mid-quality countries. The estimation error is also substantial, with an RMSE about half of the average true income growth. In some cases, relying on the predicted GDP growth can lead to very large errors of up to 5-6% in annualized terms in either direction, not only for the lower-quality countries (Guinea, Zimbabwe, Central African Republic) but also the higher-quality ones (Ethiopia, Uganda, Nigeria, Malawi).

The results for the Texan counties depict an even richer analysis at sub-national level. Estimation errors get larger, with an RMSE about 1.25 times the average true income growth. But the most interesting result is that the predicted GDP growth tends to overestimate the true income growth when true income growth is small or negative. This type of situation would have significant implications for an empirical application. For instance, suppose we used nightlights growth to predict GDP growth for the Rio Grande Valley counties — a region with a high share of migrant workers and many slow-growth counties, especially in its southern segment.[14] We would overestimate growth by roughly 2-3% in annualized terms for most of the counties, while at the same time underestimate it by roughly 5% for four highly performing counties. More importantly, we would estimate a positive GDP growth rate, around 2.5-3.5%, for four counties with true income growth as

[14]There are 248 counties in Texas, 25 of which are in the Rio Grande Valley (see Figure B.1).

negative as -5%.

4 Concluding Remarks

From policy evaluation to international comparisons, the availability of reliable measures of income is of paramount importance for empirical work. We want to be able to accurately infer true income growth. The augmented three-signal model we propose enhances the HSW methodology by solving the identification issue of their original approach. This improvement has relevant implications for the estimation of true income growth.

The real gain in accuracy comes from the identification stage of the model, rather than a more refined GDP growth predictive equation. When an official measure of GDP is available, especially when we have little confidence about the quality of the data, using the fully identified model to estimate true income growth is crucial. The optimal λ varies across samples and geographic level of analysis, and the augmented model can help to correctly choose the optimal λ to use to form the estimates.

However, the augmented model is also useful when an official measure of income is only partially available. The augmented model can be leveraged to enhance existing estimation procedures and to validate the estimates produced by other approaches, assessing the sign and magnitude of their potential measurement errors. The flexibility of the augmented model would accommodate other types of third signals instead of urban land cover, such as electrical power usage or cellular phone data. In principle, the model could also be applied to any other three-signal combinations that do not necessarily include official income statistics.

References

Alesina, Alberto, Stelios Michalopoulos, and Elias Papaioannou, "Ethnic Inequality," *Journal of Political Economy*, 2016, *124* (2), 428–488.

Baragwanath, Kathryn, Ran Goldblatt, Gordon Hanson, and Amit K. Khandelwal, "Detecting urban markets with satellite imagery: An application to India," *Journal of Urban Economics*, 2021, *125*, 103173. Delineation of Urban Areas.

Beyer, Robert Carl Michael, Esha Chhabra, Virgilio Galdo, and Martin G. Rama, "Measuring districts'monthly economic activity from outer space," Policy Research Working Paper Series 8523, The World Bank Jul 2018.

Bickenbach, Frank, Eckhardt Bode, Peter Nunnenkamp, and Mareike Söder, "Night lights and regional GDP," *Review of World Economics*, May 2016, *152* (2), 425–447.

Bluhm, Richard and Gordon C. McCord, "What Can We Learn from Nighttime Lights for Small Geographies? Measurement Errors and Heterogeneous Elasticities," *Remote Sensing*, 2022, *14* (5), 1–25.

Chen, X. and W. D. Nordhaus, "Using luminosity data as a proxy for economic statistics," *Proceedings of the National Academy of Sciences*, May 2011, *108* (21), 8589–8594.

Civelli, Andrea, Andrew Horowitz, and Arilton Teixeira, "Foreign aid and growth: A Sp P-VAR analysis using satellite sub-national data for Uganda," *Journal of Development Economics*, 2018, *134*, 50 – 67.

Dai, Zhaoxin, Yunfeng Hu, and Guanhua Zhao, "The suitability of different nighttime light data for GDP estimation at different spatial scales and regional levels," 2017.

Defourny, Pierre, Ines Moreau, Sophie Bontemps, Celine Lamarche, Carsten Brockmann, Martin Boettcher, Jan Wevers, Grit Kirches, and Maurizio Santoro, "ESA Land Cover Climate Change Initiative (ESA LC CCI) Annual LC maps v2.0.7: Product User Guide Version 2.0," Technical Report, European Space Agency 2017.

Dreher, Axel and Steffen Lohmann, "Aid and Growth at the Regional Level," IMF Working Papers 15/196, International Monetary Fund September 2015.

Elvidge, Christopher D., Jeffrey M. Safran, Ingrid L. Nelson, Benjamin T. Tuttle, Ruth Hobson, Kimberley E. Baugh, John B. Dietz, and Edward H. Erwin, "Area and Position Accuracy of DMSP Nighttime Lights Data," in R. S. Lunetta and J. G. Lyon, eds., *Remote Sensing and GIS Accuracy Assessment*, London: CRC Press, 2004.

Engstrom, Ryan, Jonathan Hersh, and David Newhouse, "Poverty from Space: Using High Resolution Satellite Imagery for Estimating Economic Well-being," *The World Bank Economic Review*, 07 2021, *36* (2), 382–412.

Ghosh, Tilottama, Rebecca L. Powell, Christopher D. Elvidge, Kimberly E. Baugh, Paul C. Sutton, and Sharolyn Anderson, "Shedding Light on the Global Distribution of Economic Activity," *The Open Geography Journal*, 2010, *3* (3), 148–61.

_ , Sharolyn Anderson, Rebecca L. Powell, Paul C. Sutton, and Christopher D. Elvidge, "Estimation of Mexico's Informal Economy and Remittances Using Nighttime Imagery," *Remote Sensing*, 2009, *1* (3), 418–44.

Gibson, John and Geua Boe-Gibson, "Nighttime lights and county-level economic activity in the United States: 2001 to 2019," *Remote Sensing*, 2021, *13* (14).

Goldblatt, Ran, Kilian Heilmann, and Yonatan Vaizman, "Can Medium-Resolution Satellite Imagery Measure Economic Activity at Small Geographies?

Evidence from Landsat in Vietnam," *The World Bank Economic Review*, 10 2019, *34* (3), 635–653.

Henderson, J. Vernon, Adam Storeygard, and David N Weil, "Measuring Economic Growth from Outer Space," *American Economic Review*, April 2012, *102* (2), 994–1028.

Hodler, Roland and Paul A. Raschky, "Regional Favoritism," *The Quarterly Journal of Economics*, 03 2014, *129* (2), 995–1033.

Keola, Souknilanh, Magnus Andersson, and Ola Hall, "Monitoring Economic Development from Space: Using Nighttime Light and Land Cover Data to Measure Economic Growth," *World Development*, 2015, *66*, 322 – 334.

Lehnert, Patrick, Michael Niederberger, Uschi Backes-Gellner, and Eric Bettinger, "Proxying Economic Activity with Daytime Satellite Imagery: Filling Data Gaps Across Time and Space," Economics of Education Working Paper Series 0165, University of Zurich, Department of Business Administration (IBW) Mar 2020.

Maldonado, Leonardo, "Lighting-up the economic activity of oil-producing regions: A remote sensing application," *Remote Sensing Applications: Society and Environment*, 2022, *26* (March), 100722.

Michalopoulos, Stelios and Elias Papaioannou, "National Institutions and Subnational Development in Africa," *The Quarterly Journal of Economics*, 12 2013, *129* (1), 151–213.

_ **and** _ , "Pre-Colonial Ethnic Institutions and Contemporary African Development," *Econometrica*, 2013, *81* (1), 113–152.

Pinkovskiy, Maxim and Xavier Sala i Martin, "Lights, Camera ... Income! Illuminating the National Accounts-Household Surveys Debate," *The Quarterly Journal of Economics*, 2016, *131* (2), 579–631.

_ **and** _ , "Newer Need Not be Better: Evaluating the Penn World Tables and the World Development Indicators Using Nighttime Lights," Working Paper 22216, National Bureau of Economic Research May 2016.

Storeygard, Adam, "Farther on down the Road: Transport Costs, Trade and Urban Growth in Sub-Saharan Africa," *The Review of Economic Studies*, 04 2016, *83* (3), 1263–1295.

Wang, Xuantong, Mickey Rafa, Jonathan D Moyer, Jing Li, Jennifer Scheer, and Paul Sutton, "Estimation and Mapping of Sub-National GDP in Uganda Using NPP-VIIRS Imagery," *Remote Sensing*, January 2019, p. 163.

Wu, Jiansheng, Zheng Wang, Weifeng Li, and Jian Peng, "Exploring factors affecting the relationship between light consumption and GDP based on DMSP/OLS nighttime satellite imagery," *Remote Sensing of Environment*, 2013, *134*, 111 – 119.

Zhang, Xiaoxuan and John Gibson, "Using Multi-Source Nighttime Lights Data to Proxy for County-Level Economic Activity in China from 2012 to 2019," *Remote Sensing*, 2022, *14* (5).

Tables and Figures

Table 1: GDP Growth (g) Predictive Regressions

	World (1)	Africa (2)	U.S. Counties (3)
l	0.389	0.201	0.575
	(0.062)	(0.105)	(0.037)
u	0.227	0.320	0.068
	(0.080)	(0.147)	(0.013)
N	178	45	2999
$adj.R^2$	0.439	0.206	0.357
$adj.R^2 - HSW$	0.395	0.155	0.355
$Period$	$1995-2019$	$2001-2019$	$2002-2020$

Note: Growth rates are calculated as log-differences over the sample. The $adj.R^2 - HSW$ is the adjusted R^2 of the HSW two-signal version of the model. Robust standard errors in parentheses.

Table 2: Signal Correlations and Model Parameters

	$corr(g,l)$	$corr(g,u)$	$corr(l,u)$	ϕ	λ^*
All Countries	0.63	0.42	0.34	0.78	0.60
– High-quality stat. capacity				0.94	0.88
– Low-quality stat. capacity				0.38	0.20
African Countries	0.42	0.35	0.22	0.65	0.54
U.S. Counties	0.59	0.16	0.12	0.81	0.70

Note: Signal correlation structure and estimates of λ^* (the optimal GDP growth weight in 10) and ϕ (the signal-to-noise ratio of the GDP growth signal defined in 6) in the augmented model for the three samples of analysis. A common correlation structure is maintained across the two sub-sets of high- and low-quality statistical capacity countries.

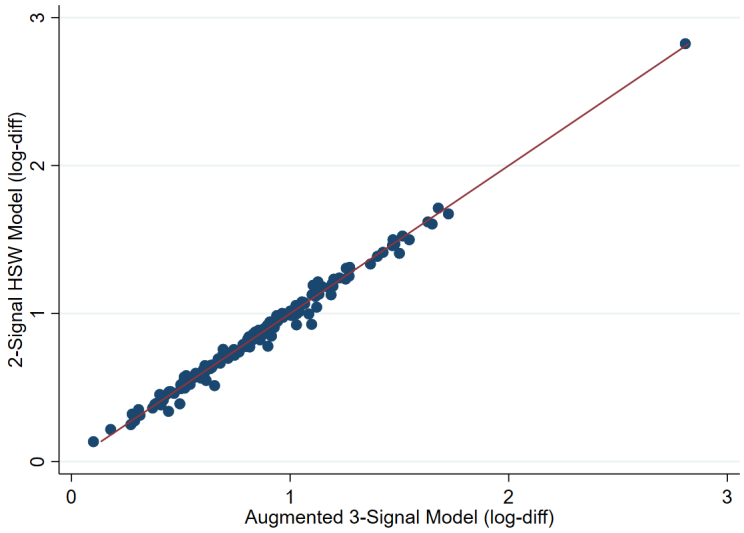

Note: Comparison of the estimated true economic activity growth $\hat{y}_i$ obtained form (4) for the augmented model (with l and u signals) with that obtained from the HSW two-signal version of the model (with l only), after attaining full identification from the three-signal model and using the subset $(\sigma_y^2, \sigma_1^2, \sigma_2^2, \beta_l)$ of those parameters to identify the two-signal model. The solid line is the 45-degree line.

Figure 1: True Growth Estimates: Two- v. Three-Signal Model

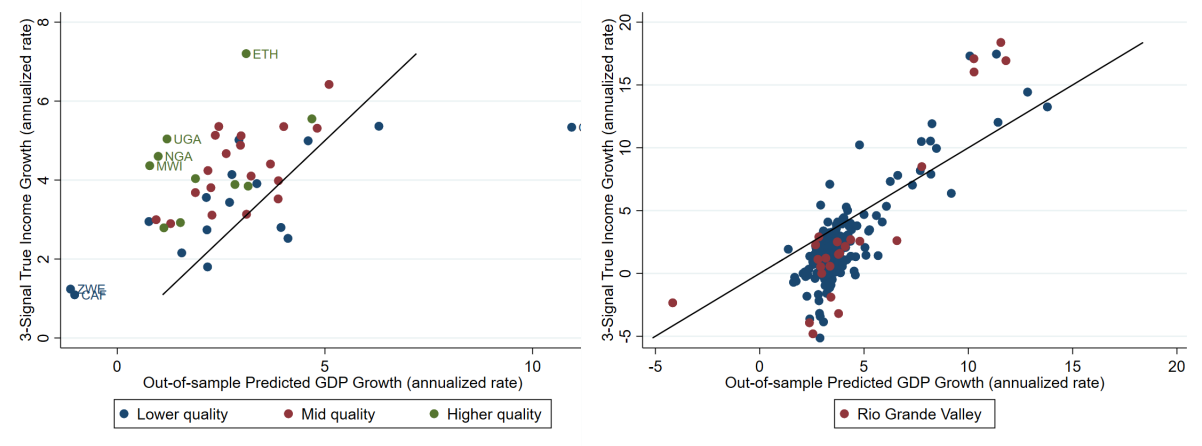

(a) African Countries

(b) Texas Counties

Note: Two thirds of observations are selected as a training sample to estimate $\hat{\psi}_l$. The coefficient is then used to predict GDP growth for the remaining "out-of-sample" observations. Average predicted GDP growth is reported out of one hundred repetitions. The solid line is the 45-degree line.

Figure 2: Light-based Predicted GDP Growth v. Three-Signal Estimated True Income Growth

Online Appendix

A Theoretical Methods

We provide in this appendix some more details about the results discussed in Section 2 of the main paper.

A.1 Solution of the Augmented Model and Empirical Requirements

In this section, we derive the solution of the augmented model and illustrate the set of technical conditions that must be empirically satisfied by the signals used in the model to obtain a solution for the parameters of the model.

The Solution: The identifying moment conditions derived in the paper (equations 11-16) are:

$$\sigma_g^2 = \sigma_y^2 + \sigma_1^2 \tag{A.1}$$

$$\sigma_l^2 = \beta_l^2 \sigma_y^2 + \sigma_2^2 \tag{A.2}$$

$$\sigma_u^2 = \beta_u^2 \sigma_y^2 + \sigma_3^2 \tag{A.3}$$

$$\sigma_{gl} = \beta_l \sigma_y^2 \tag{A.4}$$

$$\sigma_{gu} = \beta_u \sigma_y^2 \tag{A.5}$$

$$\sigma_{lu} = \beta_l \beta_u \sigma_y^2. \tag{A.6}$$

From the last three moment conditions (A.4)-(A.6), we can obtain the solution for β_l, β_u, and σ_y^2:

$$\sigma_y^2 = \frac{\sigma_{gu}\sigma_{gl}}{\sigma_{lu}} \tag{A.7}$$

$$\beta_l = \frac{\sigma_{lu}}{\sigma_{gu}} \tag{A.8}$$

$$\beta_u = \frac{\sigma_{lu}}{\sigma_{gl}}. \tag{A.9}$$

Using these solutions into (A.1)-(A.3), we find the solution for the remaining three parameters:

$$\sigma_1^2 = \sigma_g^2 - \frac{\sigma_{gu}\sigma_{gl}}{\sigma_{lu}} \tag{A.10}$$

$$\sigma_2^2 = \sigma_l^2 - \sigma_{gl}^2 \tag{A.11}$$

$$\sigma_3^2 = \sigma_u^2 - \sigma_{gu}^2. \tag{A.12}$$

Technical Requirements: There are four empirical requirements for a solution to exist. First, a third signal must be positively correlated with the second one. The relation between signals and true economic activity can be normalized, without loss of generality, to be positive, that is $\beta_l, \beta_u > 0$. This implies that σ_{gl} and σ_{gu} must be positive in (A.4)-(A.5). Therefore, given the solution for σ_y^2, also

$$\sigma_{lu} > 0. \tag{A.13}$$

The other three requirements come from (A.10)-(A.12):

$$\sigma_g^2 > \frac{\sigma_{gu}\sigma_{gl}}{\sigma_{lu}} \tag{A.14}$$

$$\sigma_l^2 > \sigma_{gl}^2 \tag{A.15}$$

$$\sigma_u^2 > \sigma_{gu}^2. \tag{A.16}$$

These three conditions simply require that the three signals exhibit sufficiently high variance relative to the observed signal covariance structure. While we find

that conditions (A.15) and (A.16) are generally easily satisfied by the data, condition (A.14) more closely depends on the covariance between second and third signals. The higher σ_{lu}, the easier the requirement is satisfied. Hence, a positive and sufficiently strong covariance between second and third signals is the key condition to empirically select the third signal.

A.2 Solution for the Split-Sample Model

We turn next to the solution for the split-sample approach discussed in Section 2 — especially in footnote 5 — and used in Section 3.3 for the heterogeneity analysis by data quality.

Let us suppose that a sample of countries can be split into two group, A and B, based on some characteristics which provides some useful information for identification. In their split-sample exercise, HSW assume that the two groups share the same model equations, except for equation (1) in which the variance of the g signal is allowed to be group specific. The identifying condition (A.1) can be restated as

$$\sigma_{g,A}^2 = \sigma_y^2 + \sigma_{1,A}^2 \tag{A.17}$$

$$\sigma_{g,B}^2 = \sigma_y^2 + \sigma_{1,B}^2. \tag{A.18}$$

This assumption also implies that equation (6), the signal to noise ratio of the g signal (i.e., GDP growth in all these applications), must differ by group:

$$\phi_A = \frac{\sigma_y^2}{\sigma_y^2 + \sigma_{1,A}^2} \tag{A.19}$$

$$\phi_B = \frac{\sigma_y^2}{\sigma_y^2 + \sigma_{1,B}^2}. \tag{A.20}$$

By calibrating ϕ_A, an additional condition is provided to solve the HSW's model for group A. In particular σ_y^2 and $\sigma_{1,A}^2$ are obtained. Given σ_y^2, (A.18) pins down $\sigma_{1,B}^2$ and, as a consequence, ϕ_B as well. This is sufficient to also find a solu-

tion of the two-signal HSW model for group B. The same approach would apply to the augmented three-signal model, but it is not necessary to find a solution in this case, as the augmented model would already be fully identified for each group separately.

Exploiting this approach, however, the augmented model allows for a further result as we discuss in the main text of the paper. Suppose a third signal u is available for group A, but not group B. The augmented model allows us to solve for all the model parameters for group A, especially σ_y^2. Under the assumption of the split-sample approach that σ_y^2 is common across groups, the two-signal model with only signals g and l for group B can be completely identified since only three parameters are left now $(\sigma_1^2, \sigma_2^2, \beta_l)$ with three moment conditions. Moreover, in this case, the remaining parameters could be taken as common across the entire sample (estimating the two-signal model with data from groups A and B) or could even be assumed to be group-specific for group A if preferred.

B Additional Tables and Figures

Table B.1: Model Parameters and the Signal Covariance Structure

Panel A: Parameter Estimations						
Model	β_l	β_u	σ_1	σ_2	σ_3	σ_y
All Countries	1.16	0.54	0.04	0.19	0.15	0.15
– High-quality statistics	1.16	0.54	0.25	0.19	0.15	0.15
– Low-quality statistics	1.16	0.54	0.01	0.19	0.15	0.15
African Countries	1.14	0.44	0.03	0.21	0.05	0.06
U.S. Counties	0.74	0.28	0.02	0.07	0.23	0.10
Panel B: Signal Covariance Structure						
Model	σ_g^2	σ_l^2	σ_u^2	σ_{gl}	σ_{gu}	σ_{lu}
All Countries	0.19	0.39	0.19	0.17	0.08	0.09
– High-quality statistics	0.16					
– Low-quality statistics	0.39					
African Countries	0.09	0.29	0.06	0.07	0.03	0.03
U.S. Counties	0.12	0.13	0.24	0.07	0.03	0.02

Note: Panel A reports the estimates of the six parameters of the augmented model. Panel B reports the covariance structures of the signals for the three cases analyzed: all countries, African countries, and U.S. counties. High-quality and Low-quality respectively indicate the set of countries with high- and Low-quality GDP data in the world countries sample. A common covariance structure is maintained across these two sub-sets, with the exception of σ_g^2.

Table B.2: Statistical Capacity of All Countries

Country	Code	Statistical Capacity Score	Low-quality	High-quality
Aruba	ABW	0	1	
Angola	AGO	46	1	
Albania	ALB	70		1
Andorra	AND	100		1
United Arab Emirates	ARE	100		1
Argentina	ARG	87		1
Armenia	ARM	92		1
Antigua and Barbuda	ATG	42	1	
Australia	AUS	100		1
Austria	AUT	100		1
Azerbaijan	AZE	79		1
Burundi	BDI	54		1
Belgium	BEL	100		1
Benin	BEN	56		1
Burkina Faso	BFA	62		1
Bangladesh	BGD	69		1
Bulgaria	BGR	91		1
Bahrain	BHR	100		1
Bahamas	BHS	100		1
Bosnia and Herzegovina	BIH	62		1
Belarus	BLR	86		1
Belize	BLZ	61		1
Bermuda	BMU	100		1
Bolivia	BOL	67		1
Brazil	BRA	83		1
Barbados	BRB	0	1	
Brunei	BRN	100		1
Bhutan	BTN	76		1
Botswana	BWA	60		1
Central African Republic	CAF	56		1
Switzerland	CHE	100		1
Chile	CHL	94		1
China	CHN	66		1
Côte d'Ivoire	CIV	59		1
Cameroon	CMR	67		1
Democratic Republic of the Congo	COD	36	1	
Republic of Congo	COG	54		1

Statistical Capacity of All Countries (continued)

Country	Code	Statistical Capacity Score	Low-quality	High-quality
Colombia	COL	84		1
Comoros	COM	50	1	
Cape Verde	CPV	73		1
Costa Rica	CRI	77		1
Cuba	CUB	99		1
Cyprus	CYP	100		1
Czech Republic	CZE	99		1
Germany	DEU	100		1
Dominica	DMA	47	1	
Denmark	DNK	100		1
Dominican Republic	DOM	68		1
Algeria	DZA	59		1
Ecuador	ECU	82		1
Egypt	EGY	86		1
Spain	ESP	100		1
Estonia	EST	99		1
Ethiopia	ETH	80		1
Finland	FIN	100		1
Fiji	FJI	53		1
France	FRA	100		1
Micronesia	FSM	28	1	
Gabon	GAB	40	1	
United Kingdom	GBR	100		1
Georgia	GEO	96		1
Ghana	GHA	66		1
Guinea	GIN	58		1
Gambia	GMB	68		1
Guinea-Bissau	GNB	46	1	
Equatorial Guinea	GNQ	32	1	
Greece	GRC	100		1
Grenada	GRD	43	1	
Guatemala	GTM	86		1
Guyana	GUY	53		1
Hong Kong	HKG	100		1
Honduras	HND	76		1
Croatia	HRV	84		1
Haiti	HTI	42	1	

Statistical Capacity of All Countries (continued)

Country	Code	Statistical Capacity Score	Low-quality	High-quality
Hungary	HUN	87		1
Indonesia	IDN	87		1
Isle of Man	IMN	100		1
India	IND	81		1
Ireland	IRL	100		1
Iran	IRN	71		1
Iraq	IRQ	41	1	
Israel	ISR	100		1
Italy	ITA	100		1
Jamaica	JAM	74		1
Jordan	JOR	77		1
Japan	JPN	100		1
Kazakhstan	KAZ	96		1
Kenya	KEN	62		1
Kyrgyzstan	KGZ	89		1
Cambodia	KHM	73		1
Kiribati	KIR	37	1	
Saint Kitts and Nevis	KNA	61		1
South Korea	KOR	100		1
Kuwait	KWT	100		1
Laos	LAO	70		1
Lebanon	LBN	57		1
Saint Lucia	LCA	60		1
Sri Lanka	LKA	77		1
Lesotho	LSO	66		1
Lithuania	LTU	99		1
Luxembourg	LUX	100		1
Latvia	LVA	99		1
Macao	MAC	0	1	
Morocco	MAR	78		1
Moldova	MDA	84		1
Madagascar	MDG	68		1
Maldives	MDV	66		1
Mexico	MEX	86		1
Marshall Islands	MHL	41	1	
Macedonia	MKD	79		1
Mali	MLI	63		1

Statistical Capacity of All Countries (continued)

Country	Code	Statistical Capacity Score	Low-quality	High-quality
Malta	MLT	100		1
Myanmar	MMR	52		1
Mongolia	MNG	74		1
Mozambique	MOZ	72		1
Mauritania	MRT	62		1
Mauritius	MUS	70		1
Malawi	MWI	79		1
Malaysia	MYS	80		1
Namibia	NAM	52		1
Niger	NER	68		1
Nigeria	NGA	69		1
Nicaragua	NIC	76		1
Netherlands	NLD	100		1
Norway	NOR	100		1
Nepal	NPL	64		1
New Zealand	NZL	100		1
Oman	OMN	0	1	
Pakistan	PAK	77		1
Panama	PAN	79		1
Peru	PER	81		1
Philippines	PHL	89		1
Papua New Guinea	PNG	41	1	
Poland	POL	86		1
Puerto Rico	PRI	100		1
Portugal	PRT	100		1
Paraguay	PRY	70		1
Palestina	PSE	42	1	
French Polynesia	PYF	0	1	
Romania	ROU	96		1
Russia	RUS	88		1
Rwanda	RWA	68		1
Saudi Arabia	SAU	100		1
Sudan	SDN	44	1	
Senegal	SEN	73		1
Singapore	SGP	100		1
Solomon Islands	SLB	40	1	
Sierra Leone	SLE	52		1

Statistical Capacity of All Countries (continued)

Country	Code	Statistical Capacity Score	Low-quality	High-quality
El Salvador	SLV	91		1
Serbia	SRB	76		1
Suriname	SUR	71		1
Slovakia	SVK	83		1
Slovenia	SVN	99		1
Sweden	SWE	100		1
Swaziland	SWZ	68		1
Seychelles	SYC	59		1
Chad	TCD	57		1
Togo	TGO	51		1
Thailand	THA	80		1
Tajikistan	TJK	74		1
Turkmenistan	TKM	39	1	
Tonga	TON	59		1
Trinidad and Tobago	TTO	71		1
Tunisia	TUN	79		1
Turkey	TUR	84		1
Tanzania	TZA	68		1
Uganda	UGA	70		1
Ukraine	UKR	88		1
Uruguay	URY	96		1
United States	USA	100		1
Uzbekistan	UZB	61		1
Saint Vincent and the Grenadines	VCT	54		1
Vietnam	VNM	64		1
Vanuatu	VUT	42	1	
Yemen	YEM	49	1	
South Africa	ZAF	82		1
Zambia	ZMB	58		1
Zimbabwe	ZWE	51		1

Note: List of countries in the world sample. The statistical capacity score is provided by the World Bank for developing countries. We assign a score of 100 by default to developed countries. A cutoff of 50 is used to classify countries as low/high quality.

Table B.3: Statistical Capacity of Included African Countries

Country	Code	Statistical Capacity Score	Low Quality	Medium Quality	High Quality
Angola	AGO	46	1		
Burundi	BDI	54	1		
Benin	BEN	56	1		
Burkina Faso	BFA	62		1	
Botswana	BWA	60		1	
Central African Republic	CAF	56	1		
Côte d'Ivoire	CIV	59		1	
Cameroon	CMR	67		1	
Democratic Rep. of Congo	COD	36	1		
Republic of Congo	COG	54	1		
Algeria	DZA	59		1	
Egypt	EGY	86			1
Ethiopia	ETH	80			1
Gabon	GAB	40	1		
Ghana	GHA	66		1	
Guinea	GIN	58		1	
Gambia	GMB	68		1	
Guinea-Bissau	GNB	46	1		
Equatorial Guinea	GNQ	32	1		
Kenya	KEN	62		1	
Liberia	LBR	33	1		
Libya	LBY	41	1		
Lesotho	LSO	66		1	
Morocco	MAR	78			1
Madagascar	MDG	68		1	
Mali	MLI	63		1	
Mozambique	MOZ	72			1
Mauritania	MRT	62		1	
Malawi	MWI	79			1
Namibia	NAM	52	1		
Niger	NER	68		1	
Nigeria	NGA	69			1
Rwanda	RWA	68		1	
Sudan	SDN	44	1		
Senegal	SEN	73			1
Sierra Leone	SLE	52	1		
Swaziland	SWZ	68		1	
Chad	TCD	57		1	
Togo	TGO	51	1		
Tunisia	TUN	79			1
Tanzania	TZA	68		1	
Uganda	UGA	70			1
South Africa	ZAF	82			1
Zambia	ZMB	58		1	
Zimbabwe	ZWE	51	1		

Note: List of countries in the African sample. The statistical capacity score is provided by the World Bank for developing countries. The quality groups are defined by the terciles of the score distribution.

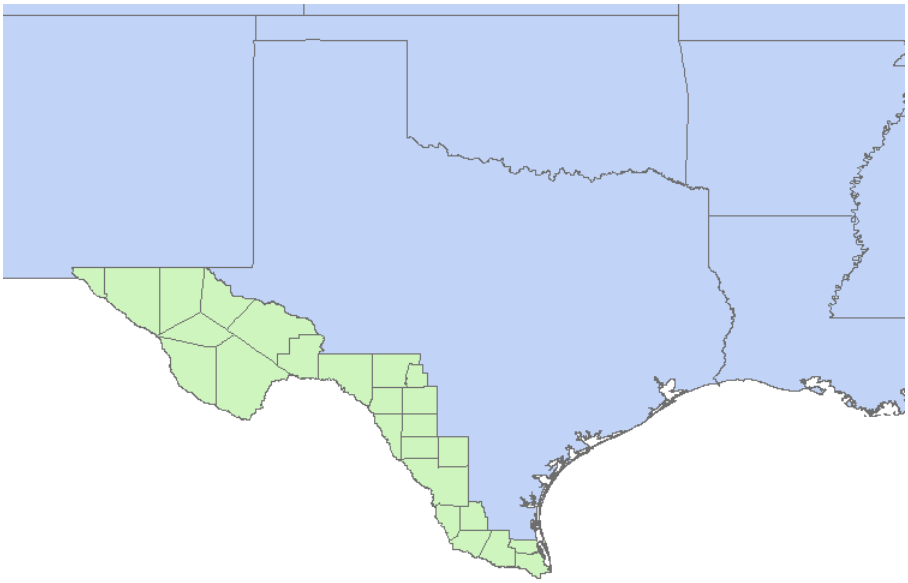

Figure B.1: Included Counties in the Rio Grande Valley sample: Cameron, Willacy, Hidalgo, Starr, Zapata, Jim Hogg, Webb, La Salle, Dimmit, Zavala, Maverick, Uvalde, Kimey, Real, Edwards, Val Verde, Terrell, Pecos, Reeves, Brewster, Presidio, Jeff Davis, Culberson, Hudspeth, El Paso